Resonance fluorescence in radiative collisions: Theoretical study of the spectral line shapes

Roberto Buffa
Dipartimento di Fisica, Università di Firenze, Largo Enrico Fermi 2, 50125 Firenze, Italy

Manlio Matera
Istituto di Elettronica Quantistica, Consiglio Nazionale delle Ricerche, Via Panciatichi 56/30, 50127 Firenze, Italy

(Received 27 March 1991)

We describe the spectral properties of the resonance fluorescence emitted in radiative collisions. The line shapes of the anelastic components of the spectrum are found to be strongly asymmetric, with extended wings related to the van der Waals shift of atomic levels. The specific case of europium and strontium atoms is considered for a combined collisional-radiative interaction following adiabatic dynamics.

PACS number(s): 32.80.−t, 34.50.Rk

I. INTRODUCTION

Radiative collisions are usually described by the general reaction

$$A_i + B_i + n\hbar\Omega \rightarrow A_f + B_f + (n \pm 1)\hbar\Omega \tag{1.1}$$

where $A_{i,f}$ and $B_{i,f}$ denote initial and final states of the atoms (or molecules) A and B, colliding in the presence of a monochromatic laser field with n photons of frequency Ω. Among atomic radiative collisions, laser-induced collisional energy transfer (LICET) has been extensively studied both theoretically and experimentally [1–17]. The process is described by the reaction

$$A^* + B + \hbar\Omega \rightarrow A + B^* \tag{1.2}$$

where the asterisks denote electronic excited states of the two atoms and the laser frequency Ω is near resonant with the interatomic transition frequency $\Omega_0 = [E(B^*) - E(A^*)]/\hbar$. Up to now the LICET process has been studied from the viewpoint of evaluating the cross section of reaction (1.2) as a function of the laser frequency Ω (excitation spectrum). The process, proposed by Gudzenko and Yakovlenko in 1972 [1], was observed for the first time by Harris and co-workers in 1977 [3]. However, only recently have improvements of the measurement accuracy [13,16,17] as well as progress in the development of theoretical models [11,15] provided an agreement between experimental and theoretical results over the full line shape of the excitation spectrum [17], leading to a deep understanding of the dynamics underlying the LICET reaction. In fact, the comparison between theory and experiment has confirmed, to the present accuracy, the validity of the basic assumptions of the models: (i) the atomic trajectories are assumed classical and rectilinear; (ii) the laser field, assumed constant during the collision, is described classically; (iii) the collisional interaction is described by a scalar dipole-dipole potential; and (iv) the magnetic degeneracy of the states involved in the transitions is neglected.

The process is conveniently described in terms of adiabatic quasimolecular states, considering the interatomic transition taking place in (1.2) as due to a transfer of energy from a doublet of states of a transient molecule, which is formed during the collision, to a final state. The resulting excitation spectrum $\sigma(\Omega)$, peaked at $\Omega = \Omega_0$, shows a strongly asymmetric shape, with an antistatic side falling off to zero very rapidly and a static wing, extending over a wider range of laser frequencies, following the double-slope law:

$$\sigma(\Omega) \propto |\Omega - \Omega_0|^{-1/2} (|\Omega - \Omega_0| + \Delta)^{-3/2} \tag{1.3}$$

where Δ is the frequency difference between the quasimolecular states at infinite interatomic separation.

Among other radiative processes of a transient molecule interacting with a laser field, near-resonant scattering appears to be of some interest. In a very recent paper [18], to be referred to as BM, we have presented a theoretical study of the resonance fluorescence spectrum emitted by a collisional pair during a LICET reaction. Following an adiabatic dressed-state approach, a seven-peak spectral structure was predicted. Some of the spectral lines were found to be due to emission processes taking place only during the collision, allowing a characterization of the process as resonance fluorescence of a transient molecule. In this paper we proceed with the theoretical investigation of the process with the aim of showing how the line shapes of the anelastic components of the spectrum are related to the collisional dynamics. We will refer to the specific case of collisions between europium and strontium atoms, for which an extensive investigation has been carried out for the measurement of the excitation spectrum [13,16,17] and work is in progress to observe the resonance fluorescence spectrum.

After reviewing the model introduced in BM (Sec. II), we proceed in Sec. III with an analysis of the interaction dynamics based on an adiabatic approximation, providing explicit expressions for the spectral components of the emitted fluorescence. In Sec. IV we treat the case of a weak-field excitation and we derive analytical expres-

sions, valid in the wings of the spectral line shapes, by using the method of the stationary phase. In Sec. V we present the results of numerical calculations to show the validity of the approximations used in the preceding sections. Finally, in the Appendix, we detail the calculations relative to the stationary phase method.

II. THE MODEL

A diagram of the relevant energy levels of the europium and strontium atoms involved in the LICET process is shown in Fig. 1. The Eu atom, prepared in the $(6s6p)\,^8P_{9/2}$ excited state at 21 767 cm^{-1}, undergoes a collision with the Sr atom in the $(5s^2)\,^1S_0$ ground state in the presence of a monochromatic laser field, nearly resonant with the interatomic transition $Eu(6s6p)\,^8P_{9/2} \rightarrow Sr(5p^2)\,^1D_2$. Due to the absorption of a photon of energy $\hbar\Omega$ from the laser field, the excitation energy of the Eu atom is transferred during the collision to the Sr atom, which is then left in the excited state $(5p^2)\,^1D_2$ at 36 970 cm^{-1}. Since the $Sr(5s5p)\,^1P_1$ excited state at 21 704 cm^{-1} is nearly resonant with the $Eu(6s6p)\,^8P_{9/2}$ initial state, one channel of excitation dominates the process which is then conveniently studied in the following product-state basis:

$$
\begin{aligned}
|i\rangle &= |\mathrm{Eu}(6s6p)\,^8P_{9/2}\rangle|\mathrm{Sr}(5s^2)\,^1S_0\rangle\ , \\
|x\rangle &= |\mathrm{Eu}(6s^2)\,^8S_{7/2}\rangle|\mathrm{Sr}(5s5p)\,^1P_1\rangle\ , \\
|f\rangle &= |\mathrm{Eu}(6s^2)\,^8S_{7/2}\rangle|\mathrm{Sr}(5p^2)\,^1D_2\rangle\ .
\end{aligned}
\tag{2.1}
$$

According to Refs. [11] and [15], the equations of motion for the probability amplitudes of states (2.1) are written as follows:

$$
i\dot{\mathbf{a}}(t) = \underline{H}(t)\mathbf{a}(t) \tag{2.2}
$$

with

$$
\mathbf{a}(t) = \begin{bmatrix} a_i(t) \\ a_x(t) \\ a_f(t) \end{bmatrix}\ , \tag{2.3}
$$

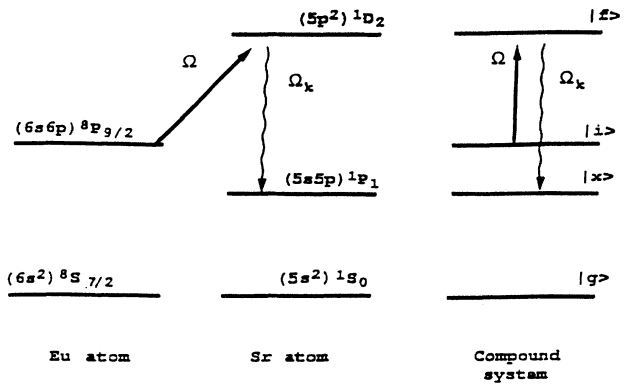

FIG. 1. Configuration of the relevant energy levels of the Eu and Sr atoms involved in the near-resonant scattering process. Energy levels of the product states are shown on the right.

$$
\underline{H}(t) = \begin{bmatrix} 0 & V(t)\exp(i\Delta t) & 0 \\ V(t)\exp(-i\Delta t) & 0 & -\chi\exp(i\delta t) \\ 0 & -\chi\exp(-i\delta t) & 0 \end{bmatrix}\ . \tag{2.4}
$$

In (2.4) $\Delta = (E_i - E_x)/\hbar = 63\ cm^{-1}$, $\delta = \Omega - (E_f - E_x)/\hbar$, and $V(t)$ and χ describe, respectively, the collisional and the atom-field interactions. As a result of the short time scale τ_c of the collision, of the order of 1–10 ps, χ is assumed constant, while $V(t)$ is well described by a dipole-dipole collisional interaction given, taking classical and rectilinear trajectories for the colliding atoms, by

$$
V(t) = d_A d_B/\hbar(b^2 + v^2t^2)^{3/2} \tag{2.5}
$$

where b is the impact parameter, v is the relative speed of the atoms, and $d_A d_B$ is the dipole-dipole interaction energy. The $Sr(5p^2)\,^1D_2$ and $Sr(5s5p)\,^1P_1$ levels are coupled by a dipole radiative transition and the Sr atom can radiate during the collision emitting a photon of energy $\hbar\Omega_k$ with decay rate γ. Since the collision takes place on a time scale much shorter than the radiative lifetime $1/\gamma$ of the $Sr(5p^2)\,^1D_2$ level, then at most one fluorescence photon per atom is emitted during the collision, and the analysis of the process is greatly simplified. In BM we have shown that the fluorescence spectrum can be written as

$$
P(\Omega_k) = \gamma \sum_{\sigma} \int_0^{+\infty} b \left| \int_{-\infty}^{+\infty} \underline{U}^{\dagger}(t)\mathbf{F}(t)dt \right|^2 db \tag{2.6}
$$

where $\underline{U}(t)$ is solution of the differential equation:

$$
i\dot{\underline{U}}(t) = \underline{H}(t)\underline{U}(t)\ , \tag{2.7}
$$

$\mathbf{F}(t)$ is given by

$$
\mathbf{F}(t) = a_f(t)\exp(i\delta_k t)\begin{bmatrix} 0 \\ 1 \\ 0 \end{bmatrix} \tag{2.8}
$$

with $\delta_k = \Omega_k - (E_f - E_x)/\hbar$, and σ represents the polarization of the emitted radiation.

III. ADIABATIC INTERACTION

By using the unitary transformation:

$$
\underline{U}_T(t) = \underline{T}(t)\underline{U}(t) \tag{3.1}
$$

with

$$
\underline{T}(t) = \begin{bmatrix} \exp(-i\Delta t) & 0 & 0 \\ 0 & 1 & 0 \\ 0 & 0 & \exp(i\delta t) \end{bmatrix} \tag{3.2}
$$

we obtain

$$
i\dot{\underline{U}}_T(t) = \underline{H}'(t)\underline{U}_T(t) \tag{3.3}
$$

with

$$
\underline{H}'(t) = \begin{bmatrix} \Delta & V(t) & 0 \\ V(t) & 0 & -\chi \\ 0 & -\chi & -\delta \end{bmatrix}\ . \tag{3.4}
$$

The Hamiltonian $\underline{H}'(t)$ can be diagonalized by the unitary transformation

$$\underline{D}(t)\underline{H}'(t)\underline{D}^{-1}(t)=\underline{\Lambda}(t) = \begin{bmatrix} \lambda_1(t) & 0 & 0 \\ 0 & \lambda_2(t) & 0 \\ 0 & 0 & \lambda_3(t) \end{bmatrix} \tag{3.5}$$

where the matrix elements $D_{jk}(t)$ of $\underline{D}(t)$ are given by

$$\begin{aligned} D_{j1}(t)&=V(t)[\lambda_j(t)+\delta]/S_j(t)\ , \\ D_{j2}(t)&=[\lambda_j(t)+\delta][\lambda_j(t)-\Delta]/S_j(t)\ , \\ D_{j3}(t)&=\chi[\Delta-\lambda_j(t)]/S_j(t) \end{aligned} \tag{3.6}$$

with

$$S_j(t)=\{V^2(t)[\lambda_j(t)+\delta]^2+[\lambda_j(t)+\delta]^2[\lambda_j(t)-\Delta]^2 +\chi^2[\Delta-\lambda_j(t)]^2\}^{1/2} \tag{3.7}$$

and where the time-dependent adiabatic eigenvalues $\lambda_j(t)$ are given by the solution of the third-order secular equation:

$$|\underline{H}'(t)-\lambda(t)\underline{I}|=0\ . \tag{3.8}$$

Transformation (3.5) leads to the definition of the time-dependent adiabatic dressed states:

$$|D_j,n\rangle=D_{j1}(t)|i\rangle|n\rangle+D_{j2}(t)|x\rangle|n\rangle +D_{j3}(t)|f\rangle|n-1\rangle \tag{3.9}$$

used in BM to predict a seven-peak structure for the spectral distribution of the scattered radiation.

The matrix $\underline{U}_D(t)$, defined by the unitary transformation

$$\underline{U}_D(t)=\underline{D}(t)\underline{U}_T(t) \tag{3.10}$$

evolves in time according to

$$i\dot{\underline{U}}_D(t)=[\underline{\Lambda}(t)+i\dot{\underline{D}}(t)\underline{D}^{-1}(t)]\underline{U}_D(t)\ . \tag{3.11}$$

For a laser detuning in the antistatic region of the excitation spectrum ($\delta+\Delta>0$) the adiabatic eigenvalues $\lambda_j(t)$ never cross and, for $\delta+\Delta\gg 1/\tau_c$, the off-diagonal terms of $\dot{\underline{D}}(t)\underline{D}^{-1}(t)$ in (3.11) become negligibly small when compared to the differences $|\lambda_j(t)-\lambda_k(t)|$ ($j\neq k$). We can therefore ignore the term in $\dot{\underline{D}}(t)\underline{D}^{-1}(t)$ in (3.11) to find the following simple solution for $\underline{U}_D(t)$:

$$\underline{U}_D(t)= \begin{bmatrix} \exp\left[-i\int_{-\infty}^{t}\lambda_1(t')dt'\right] & 0 & 0 \\ 0 & \exp\left[-\int_{-\infty}^{t}\lambda_2(t')dt'\right] & 0 \\ 0 & 0 & \exp\left[-i\int_{-\infty}^{t}\lambda_3(t')dt'\right] \end{bmatrix}. \tag{3.12}$$

No transfer of population occurs among the adiabatic dressed states (3.9) during all the interaction time, even though the bare states (2.1) can have a non-negligible fraction of population. The matrix $\underline{U}(t)$ to introduce in (2.6) assumes then the following expression:

$$\underline{U}(t)=\underline{T}^{-1}(t)\underline{D}^{-1}(t)\underline{U}_D(t) = \begin{bmatrix} D_{11}(t)\exp\left[i\int_{-\infty}^{t}[\Delta-\lambda_1(t')]dt'\right] & D_{21}(t)\exp\left[\int_{-\infty}^{t}[\Delta-\lambda_2(t')dt'\right] & D_{31}(t)\exp\left[i\int_{-\infty}^{t}[\Delta-\lambda_3(t')]dt'\right] \\ D_{12}(t)\exp\left[-i\int_{-\infty}^{t}\lambda_1(t')dt'\right] & D_{22}(t)\exp\left[-i\int_{-\infty}^{t}\lambda_2(t')dt'\right] & D_{32}(t)\exp\left[-i\int_{-\infty}^{t}\lambda_3(t')dt'\right] \\ D_{13}(t)\exp\left[-i\int_{-\infty}^{t}[\delta+\lambda_1(t')]dt'\right] & D_{23}(t)\exp\left[-i\int_{-\infty}^{t}[\delta+\lambda_2(t')]dt'\right] & D_{33}(t)\exp\left[-i\int_{-\infty}^{t}[\delta+\lambda_3(t')]dt'\right] \end{bmatrix}. \tag{3.13}$$

Since $D_{11}(-\infty)=1$ and $D_{12}(-\infty)=D_{13}(-\infty)=0$, the first column of (3.13) is the solution of (2.2) for our initial condition:

$$\mathbf{a}(-\infty)= \begin{bmatrix} 1 \\ 0 \\ 0 \end{bmatrix}$$

and

$$a_f(t)=D_{13}(t)\exp\left[-i\int_{-\infty}^{t}[\delta+\lambda_1(t')]dt'\right] \tag{3.14}$$

is the expression of $a_f(t)$ to introduce in (2.8). The fluorescence spectrum assumes then the following expression:

$$P(\Omega_k)=\gamma\sum_{\sigma}[I_{11}(\Omega_k)+I_{12}(\Omega_k)+I_{13}(\Omega_k)] \tag{3.15}$$

with

$$I_{11}(\Omega_k)=\int_0^{+\infty} b\left|\int_{-\infty}^{+\infty} W_{11}(t)\exp\left[i\int_{-\infty}^{t}(\Omega_k-\Omega)dt'\right]dt\right|^2 db\ ,$$
$$I_{12}(\Omega_k)=\int_0^{+\infty} b\left|\int_{-\infty}^{+\infty} W_{12}(t)\exp\left[i\int_{-\infty}^{t}[\Omega_k-\Omega-\lambda_1(t')+\lambda_2(t')]dt'\right]dt\right|^2 db\ , \tag{3.16}$$
$$I_{13}(\Omega_k)=\int_0^{+\infty} b\left|\int_{-\infty}^{+\infty} W_{13}(t)\exp\left[i\int_{-\infty}^{t}[\Omega_k-\Omega-\lambda_1(t')+\lambda_3(t')]dt'\right]dt\right|^2 db\ ,$$

and where

$$W_{1j}(t)=D_{13}(t)D_{j2}(t) \tag{3.17}$$

are the dimensionless radiative matrix elements that couple the dressed state $|D_1,n\rangle$ with the dressed states $|D_j,n-1\rangle$ of a lower-lying multiplet.

This spectral structure is sketched in Fig. 2, where the relative intensities are not significant. Due to the adiabatic character of the combined radiative-collisional interaction, in the seven-peak spectral structure only the lines originating from transitions starting from state $|D_1,n\rangle$ will be present. The elastic component $I_{11}(\Omega_k)$ is symmetric with a width related to the inverse of the average collision time. The anelastic lines, $I_{12}(\Omega_k)$ and $I_{13}(\Omega_k)$, are asymmetric with shapes affected by the collisional van der Waals shift. The detailed analysis of these line shapes can be of great importance for the study of the dynamics of radiative collisions.

IV. WEAK-FIELD REGIME

In the absence of the laser field, the Hamiltonian (3.4) describes the collisional interaction between Eu and Sr atoms. It is shown in Refs. [11] and [15] that, since the condition

$$|\dot{V}(t)/V(t)|\ll\Delta \tag{4.1}$$

is satisfied, the time evolution of the colliding atoms is well described by adiabatic collisional dressed states defined by

$$|+\rangle=(\cos\theta)|i\rangle+(\sin\theta)|x\rangle\ ,$$
$$|-\rangle=(\cos\theta)|x\rangle-(\sin\theta)|i\rangle \tag{4.2}$$

with $\tan(2\theta)=2V(t)/\Delta$. The collisional dressed states (4.2) are quasimolecular states with adiabatic time-dependent eigenvalues given by

$$\lambda_+(t)=(\Delta/2)(1+\{1+[2V(t)/\Delta]^2\}^{1/2})\ ,$$
$$\lambda_-(t)=(\Delta/2)(1-\{1+[2V(t)/\Delta]^2\}^{1/2})\ . \tag{4.3}$$

For a weak laser field we can write the Hamiltonian (3.4) as

$$\underline{H}'(t)=\underline{H}_0(t)+\underline{H}_1(t) \tag{4.4}$$

with

$$\underline{H}_0(t)=\begin{bmatrix}\Delta & V(t) & 0\\ V(t) & 0 & 0\\ 0 & 0 & -\delta\end{bmatrix} \tag{4.5}$$

and

$$\underline{H}_1(t)=\begin{bmatrix}0 & 0 & 0\\ 0 & 0 & -\chi\\ 0 & -\chi & 0\end{bmatrix}\ , \tag{4.6}$$

and treat $\underline{H}_1(t)$ as a perturbation, to obtain the expressions of all the relevant quantities of Sec. III to the lowest order in χ. In particular, the matrix elements (3.17) reduce to

$$W_{11}(t)\approx-\chi\sin^2\theta/[\delta+\lambda_+(t)]\ ,$$
$$W_{12}(t)=-\chi\sin\theta\cos\theta/[\delta+\lambda_+(t)]\ , \tag{4.7}$$
$$W_{13}(t)\approx\frac{-\chi^2(\sin\theta)(\Delta+\delta)}{[\delta+\lambda_+(t)]^2[\delta+\lambda_-(t)]}\ ,$$

and the three spectral components (3.16) to

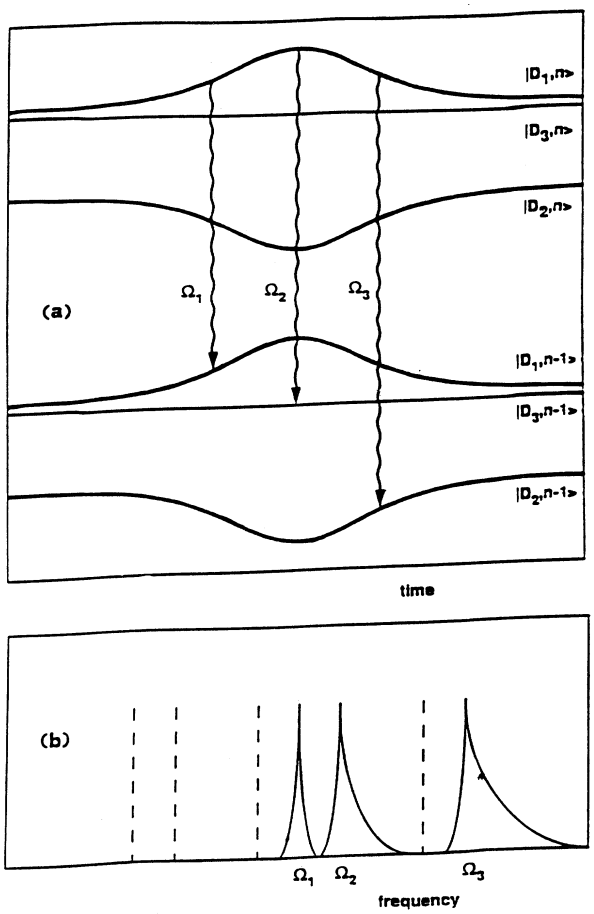

FIG. 2. Structure of the resonance fluorescence spectrum for adiabatic collisional-radiative interaction: (a) spontaneous emission transition from dressed state $|D_1,n\rangle$; (b) corresponding spectrum, showing the collision-induced wings.

$$I_{11}(\Omega_k)\approx I_R(\Omega_k)=\chi^2\int_0^{+\infty}b\left|\int_{-\infty}^{+\infty}\{\sin^2\theta/[\delta+\lambda_+(t)]\}\exp\left[i\int_{-\infty}^{t}(\Omega_k-\Omega)dt'\right]dt\right|^2db\ , \tag{4.8a}$$

$$I_{12}(\Omega_k)\approx I_{AS}(\Omega_k)=\chi^2\int_0^{+\infty}b\left|\int_{-\infty}^{+\infty}\{\sin\theta\cos\theta/[\delta+\lambda_+(t)]\}\right.$$
$$\left.\times\exp\left[i\int_{-\infty}^{t}[\Omega_k-\Omega+\lambda_-(t)-\lambda_+(t)]dt'\right]dt\right|^2db\ , \tag{4.8b}$$

$$I_{13}(\Omega_k)\approx I_{3P}(\Omega_k)=\chi^4\int_0^{+\infty}b\left|\int_{-\infty}^{+\infty}(\sin\theta)(\Delta+\delta)/\{[\delta+\lambda_+(t)]^2[\delta+\lambda_-(t)]\}\right.$$
$$\left.\times\exp\left[i\int_{-\infty}^{t}[\Omega_k-\Omega-\delta-\lambda_+(t)]dt'\right]dt\right|^2db\ . \tag{4.8c}$$

The three spectral features appearing in (4.8) have been recognized in BM as Rayleigh (4.8a), anti-Stokes (4.8b), and three-photon (4.8c) components, centered, respectively, at $\Omega_k=\Omega$, $\Omega_k=\Omega+\Delta$, and $\Omega_k=\Omega+\delta+\Delta$.

The major contribution to the integrals over time appearing in (4.8b) and (4.8c) comes from the two points at which the phase is stationary and the frequency difference between the emitted photon and the excitation laser photon is equal to the transition frequency between the quasimolecular states involved in the scattering process, i.e.,

$$\Omega_k-\Omega=\lambda_+(t)-\lambda_-(t)$$

for the anti-Stokes component (4.8b), and

$$\Omega_k-\Omega=\lambda_+(t)+\delta$$

for the three-photon component (4.8c). Therefore these integrals can be approximately evaluated by using the method of stationary phase [19], followed in Refs. [11] and [15] to obtain the far-wing behavior of the excitation spectrum (1.3). Details of the calculation are reported in the Appendix. The final result is that the anti-Stokes (4.8b) and three-photon (4.8c) components of the fluorescence spectrum follow in the wing analytical laws given, respectively, by

$$I_{AS}(\Omega_k)\approx\chi^2(\pi d_A d_B/3\hbar v)(8/\{(\Delta+\Delta_k)[\Delta_k+2(\delta+\Delta)]^2[\Delta_k(\Delta_k+2\Delta)]^{1/2}\})\ , \tag{4.9}$$

$$I_{3P}(\Omega_k)\approx\chi^4(2\pi d_A d_B/3\hbar v)\{(\delta+\Delta)^2/[(\delta+\Delta+\Delta_k)^4(\delta-\Delta_k)^2\Delta_k^{1/2}(\Delta_k+\Delta)^{3/2}]\} \tag{4.10}$$

where $\Delta_k=\Omega_k-\Omega_0$ is the detuning of the emitted photon from the respective line centers Ω_0. Expressions (4.9) and (4.10) are plotted in Fig. 3 for the specific case $\delta+\Delta=10$ cm^{-1} and compared with the double-slope function (1.3).

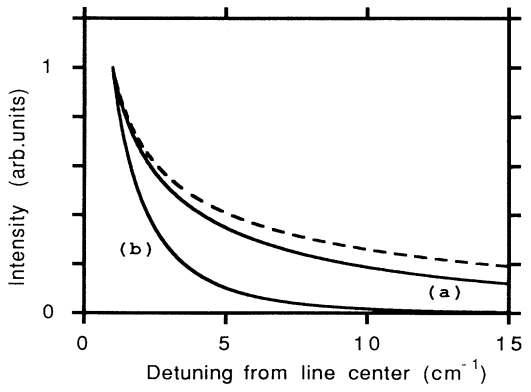

FIG. 3. Wings of the spectral line shapes of the (a) anti-Stokes and (b) three-photon components, plotted for $\delta+\Delta=10$ cm^{-1} and compared with the double-slope line shape of the excitation spectrum (1.3) (dashed line). Data have been normalized to 1 at a detuning from line center of 1 cm^{-1}.

V. NUMERICAL RESULTS

Numerical calculations have been performed with the aim of checking directly the validity of the adiabatic and stationary phase approximations used in the preceding section to obtain the analytical line shapes (4.9) and (4.10) for the anti-Stokes and three-photon components of the fluorescence spectrum. All calculations have been done taking a collisional interaction energy $d_A d_B=2.17\times10^{-35}$ erg cm^3 and a relative speed of the colliding atoms $v=5\times10^4$ cm/s. The integration time was from -60 to $+60$ ps. As an example, in Fig. 4 the temporal evolution of the population of the $|f\rangle$ state, $|a_f(t)|^2$, is shown for different values of the laser detuning δ and impact parameter b for a Rabi frequency $\chi=1$ cm^{-1}. The continuous lines represent the adiabatic approximation (3.14) while the dashed lines have been obtained by numerical integration of Eq. (2.2). These calculations show that, for a laser intensity corresponding to a Rabi frequency of 1 cm^{-1}, the adiabatic approximation provides accurate results for laser detunings in the antistatic side of the excitation spectrum larger than 10 cm^{-1} ($\delta+\Delta\geq10$ cm^{-1}).

In Figs. 5 and 6 the line shapes of the anti-Stokes and three-photon components of the fluorescence spectrum

are shown. The continuous lines reproduce the analytical expressions (4.9) and (4.10) while the circles are the result of numerical calculations performed by using expression (3.16). Data refer to a laser detuning of 10 cm^{-1} in the antistatic region of the excitation spectrum ($\delta+\Delta=10$ cm^{-1}) and a Rabi frequency $\chi=1$ cm^{-1}. The comparison confirms that the stationary phase method used in Sec. IV gives excellent results in the wings of the anti-Stokes and three-photon components.

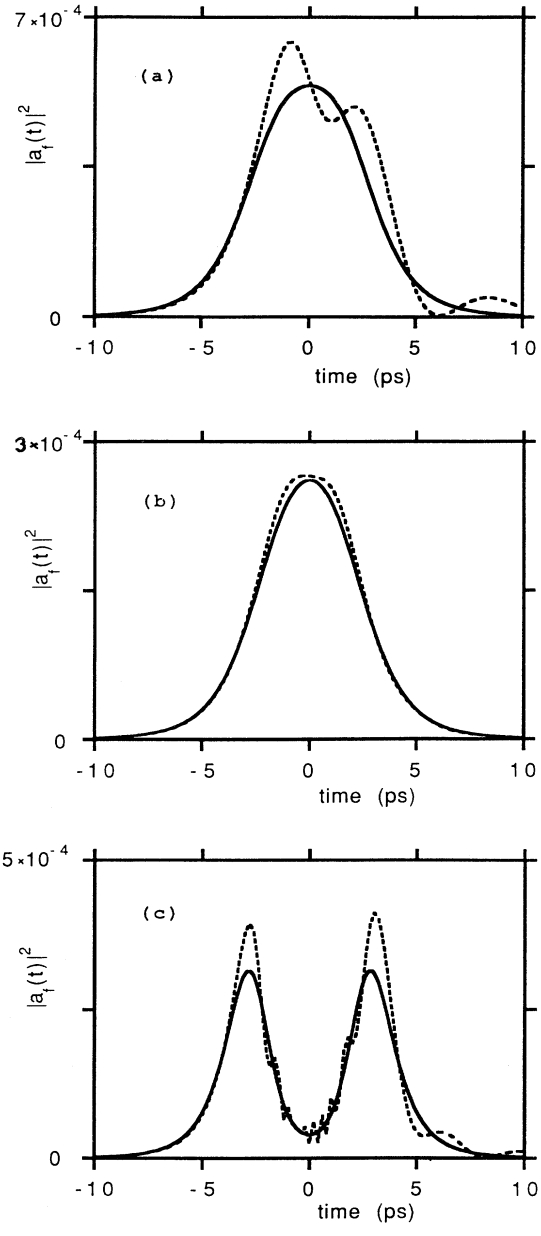

FIG. 4. Temporal evolution of the $|f\rangle$-state population $|a_f(t)|^2$. The continuous lines represent the adiabatic approximation (3.14) while the dashed lines have been obtained by numerical integration of (2.2): (a) $\chi=1$ cm^{-1}, $\delta+\Delta=6$ cm^{-1}, $b=2.0$ nm; (b) $\chi=1$ cm^{-1}, $\delta+\Delta=10$ cm^{-1}, $b=2.0$ nm; (c) $\chi=1$ cm^{-1}, $\delta+\Delta=10$ cm^{-1}, $b=1.0$ nm.

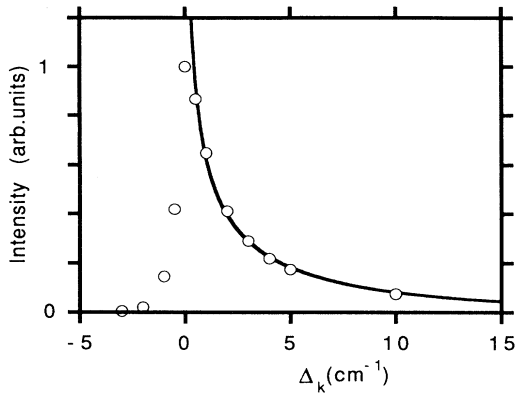

FIG. 5. Spectral line shape of the anti-Stokes component for $\chi=1$ cm^{-1} and $\delta+\Delta=10$ cm^{-1}. Circles are the result of a numerical calculation performed by using (3.16b) while the continuous line reproduces the analytical expression (4.9).

VI. CONCLUSIONS

We have presented a theoretical study of the spectrum of the resonance fluorescence emitted in a LICET process, showing how the line shapes of the anelastic components are related to the collisional dynamics. For a laser frequency tuned in the antistatic side of the excitation spectrum, the dynamics of the combined collisional-radiative interaction is found to be well described by adiabatic dressed states. The seven-peak spectral structure predicted in BM reduces, in this case, to a triplet: the elastic Rayleigh component and two anelastic features recognized as anti-Stokes and three-photon components. The anelastic components are found strongly asymmetric with wings affected by the collisional van der Waals shift. Due to the different time evolution of the eigenvalues of the quasimolecular states involved in the scattering pro-

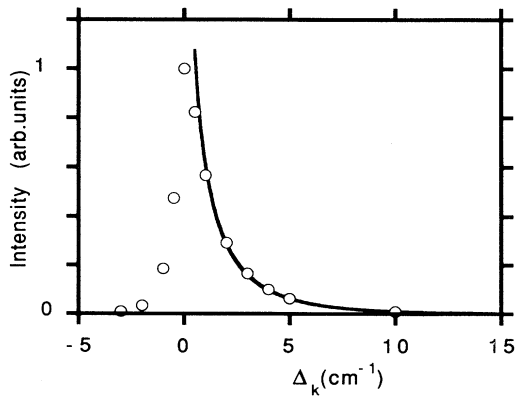

FIG. 6. Spectral line shape of the three-photon component for $\chi=1$ cm^{-1} and $\delta+\Delta=10$ cm^{-1}. Circles are the result of a numerical calculation performed by using (3.16c) while the continuous line reproduces the analytical expression (4.10).

cess, the three-photon component appears much sharper and more symmetric than the anti-Stokes component. In the case of a weak-field excitation, we have provided analytical expressions valid in the wings of the anti-Stokes and three-photon line shapes. Numerical calculations, performed for the specific case of collisions between europium and strontium atoms, confirm that the approximations used in the analysis of the process provide very accurate results. The properties of the combined collisional-radiative interaction of europium and strontium atoms, which have been extensively investigated in previous works, together with the results of this study, make this system a good candidate for the observation of the resonance fluorescence of a transient molecule.

APPENDIX

Expressions (4.8b) and (4.8c) can be written, respectively, as follows:

$$I_{AS}(\Omega_k)=\chi^2\int_{b_{min}}^{b_{max}} bF_{AS}(\Omega_k,b)db \ , \tag{A1}$$

$$I_{3P}(\Omega_k)=\chi^4\int_{b_{min}}^{b_{max}} bF_{3P}(\Omega_k,b)db \ , \tag{A2}$$

with

$$F_{AS}(\Omega_k,b)=\left|\int_{-\infty}^{+\infty}[\sin\theta\cos\theta/(\delta+\lambda_+)]\exp\left[i\int_{-\infty}^{t}(\Omega_k-\Omega-\lambda_++\lambda_-)dt'\right]dt\right|^2 , \tag{A3}$$

$$F_{3P}(\Omega_k,b)=\left|\int_{-\infty}^{+\infty}\{\sin\theta(\Delta+\delta)/[(\delta+\lambda_+)^2(\delta+\lambda_-)]\}\exp\left[i\int_{-\infty}^{t}(\Omega_k-\Omega-\lambda_+-\delta)dt'\right]dt\right|^2 , \tag{A4}$$

and where

$$\lambda_+=(\Delta/2)\{1+[1+(2V/\Delta)^2]^{1/2}\} \ , \tag{A5}$$

$$\lambda_-=(\Delta/2)\{1-[1+(2V/\Delta)^2]^{1/2}\} \ , \tag{A6}$$

$$(\sin\theta)^2=\{[1+(2V/\Delta)^2]^{1/2}-1\}/\{2[1+(2V/\Delta)^2]^{1/2}\} \ , \tag{A7}$$

$$(\cos\theta)=\{[1+(2V/\Delta)^2]^{1/2}+1\}/\{2[1+(2V/\Delta)^2]^{1/2}\} \ . \tag{A8}$$

The method of stationary phase [19] provides a means to approximately evaluate integrals (A3) and (A4), respectively, as

$$F_{AS}(\Omega_k,b)\approx(4\pi/|\ddot{\Phi}_s|)[\sin\theta_s\cos\theta_s/(\delta+\lambda_{+s})]^2 \ , \tag{A9}$$

$$F_{3P}(\Omega_k,b)\approx(4\pi/|\ddot{\Phi}_s|)\left[\frac{\sin\theta_s(\Delta+\delta)}{(\delta+\lambda_{+s})^2(\delta+\lambda_{-s})}\right]^2 \tag{A10}$$

where s indicates the points at which the phases (indicated with Φ) of the integrand functions in (A3) and (A4) are stationary, i.e., $\dot{\Phi}_s=0$. We have ignored the possible interference effects coming from the fact that stationary phase is reached at two different points.

1. Anti-Stokes component

In this case we have

$$\dot{\Phi}_s=\Omega_k-\Omega-\lambda_{+s}+\lambda_{-s}$$
$$=\Omega_k-\Omega-\Delta[1+(2V_s/\Delta)^2]^{1/2}=0 \tag{A11}$$

from where

$$\Delta[1+(2V_s/\Delta)^2]^{1/2}=\Omega_k-\Omega=\Delta_k+\Delta \tag{A12}$$

with $\Delta_k=\Omega_k-\Omega-\Delta$. Introducing (A12) in (A5), (A7), and (A8) we obtain

$$\lambda_{+s}=(\Delta_k+2\Delta)/2 \ ,$$
$$\sin\theta_s=\{\Delta_k/[2(\Delta_k+\Delta)]\}^{1/2} \ , \tag{A13}$$
$$\cos\theta_s=\{(\Delta_k+2\Delta)/[2(\Delta_k+\Delta)]\}^{1/2} \ .$$

From (A12) we also obtain

$$V_s=d_Ad_B/\hbar R_s^3=\{[\Delta_k(\Delta_k+2\Delta)]^{1/2}\}/2 \tag{A14}$$

from where

$$R_s=\{4(d_Ad_B/\hbar)^2/[\Delta_k(\Delta_k+2\Delta]\}^{1/6} \ . \tag{A15}$$

The second derivative of the phase Φ is given by

$$\ddot{\Phi}=-\left[4V\left[\frac{dV}{dR}\right]\dot{R}\right]\Big/\left\{\Delta\left[1+\left[\frac{2V}{\Delta}\right]^2\right]^{1/2}\right\} \tag{A16}$$

where

$$\frac{dV}{dR}=-\frac{3V}{R} \tag{A17}$$

and

$$\dot{R}=v[1-(b/R)^2]^{1/2} \tag{A18}$$

from where, using (A14), we obtain

$$\ddot{\Phi}_s=3v\frac{\Delta_k(\Delta_k+2\Delta)}{(\Delta_k+\Delta)}\frac{[1-(b/R_s)^2]^{1/2}}{R_s} \ . \tag{A19}$$

Introducing (A13) and (A19) in (A9) we obtain

$$F_{AS}(\Omega_k,b)\approx(4\pi/3v)(1/\{(\Delta_k+\Delta)[\Delta_k+2(\delta+\Delta)]^2\})$$
$$\times\{R_s/[1-(b/R_s)^2]^{1/2}\} \ . \tag{A20}$$

Introducing now (A20) in (A1) we obtain

$$\int_{b_{\min}}^{b_{\max}} bF_{AS}(\Omega_k,b)db \approx (4\pi/3v)(1/\{[\Delta_k+2(\delta+\Delta)]^2(\Delta+\Delta_k)\})R_s^3\int_0^1[x/(1-x^2)^{1/2}]dx \tag{A21}$$

with $x=b/R_s$ and where we set $b_{\min}=0$ and $b_{\max}=R_s$. Finally, making use of (A15) in (A21), we obtain

$$I_{AS}(\Omega_k)\approx\chi^2(\pi d_A d_B/3\hbar v)(8/\{(\Delta+\Delta_k)[\Delta_k+2(\delta+\Delta)]^2[\Delta_k(\Delta_k+2\Delta)]^{1/2}\}) . \tag{A22}$$

2. Three-photon component

In this case we have

$$\dot{\Phi}_s=\Omega_k-\Omega-\delta-\lambda_{+s}$$
$$=\Omega_k-\Omega-\delta-\Delta/2\{1+[1+(2V_s/\Delta)^2]^{1/2}\}=0 \tag{A23}$$

from where

$$\Delta[1+(2V_s/\Delta)^2]^{1/2}=2(\Omega_k-\Omega-\delta)-\Delta=2\Delta_k+\Delta \tag{A24}$$

with $\Delta_k=\Omega_k-\Omega-\delta-\Delta$. Introducing (A24) in (A5), (A6), and (A7) we obtain

$$\lambda_{+s}=\Delta_k+\Delta ,$$
$$\lambda_{-s}=-\Delta_k , \tag{A25}$$
$$\sin\theta_s=[\Delta_k/(2\Delta_k+\Delta)]^{1/2} .$$

From (A24) we also obtain

$$V_s=d_A d_B/\hbar R_s^3=[\Delta_k(\Delta_k+\Delta)]^{1/2} \tag{A26}$$

from where

$$R_s=\{(d_A d_B/\hbar)^2/[\Delta_k(\Delta_k+\Delta)]\}^{1/6} . \tag{A27}$$

The second derivative of the phase Φ is given by

$$\ddot{\Phi}=-\left[2V\left[\frac{dV}{dR}\right]\dot{R}\right]\Big/\left\{\Delta\left[1+\left[\frac{2V}{\Delta}\right]^2\right]^{1/2}\right\} \tag{A28}$$

from where, using (A17), (A18), (A24), and (A26) we obtain

$$\ddot{\Phi}_s=6v\frac{\Delta_k(\Delta_k+\Delta)}{(2\Delta_k+\Delta)}\frac{[1-(b/R_s)^2]^{1/2}}{R_s} . \tag{A29}$$

Introducing (A25) and (A29) in (A10) we obtain

$$F_{3P}(\Omega_k,b)\approx(2\pi/3v)\{(\delta+\Delta)^2/[(\delta+\Delta+\Delta_k)^4(\delta-\Delta_k)^2(\Delta_k+\Delta)]\}\{R_s/[1-(b/R_s)^2]^{1/2}\} . \tag{A30}$$

Introducing now (A30) in (A2) we obtain

$$\int_{b_{\min}}^{b_{\max}} bF_{3P}(\Omega_k,b)db \approx (2\pi/3v)\{(\Delta+\delta)^2/[(\delta+\Delta+\Delta_k)^4(\delta-\Delta_k)^2(\Delta+\Delta_k)]\}R_s^3\int_0^1[x/(1-x^2)^{1/2}]dx \tag{A31}$$

with $x=b/R_s$ and where we have set $b_{\min}=0$ and $b_{\max}=R_s$. Finally, making use of (A27) in (A31) we obtain

$$I_{3P}(\Omega_k)\approx\chi^4(2\pi d_A d_B/3\hbar v)\{(\delta+\Delta)^2/[(\delta+\Delta+\Delta_k)^4(\delta-\Delta_k)^2\Delta_k^{1/2}(\Delta_k+\Delta)^{3/2}]\} . \tag{A32}$$

[1] L. I. Gudzenko and S. I. Yakovlenko, Zh. Eksp. Teor. Fiz. **62**, 1686 (1972) [Sov. Phys.—JETP **35**, 877 (1972)].
[2] V. S. Lisitsa and S. I. Yakovlenko, Zh. Eksp. Teor. Fiz. **66**, 1550 (1974) [Sov. Phys.—JETP **39**, 759 (1974)].
[3] R. W. Falcone, W. R. Green, J. C. White, J. F. Young, and S. E. Harris, Phys. Rev. A **15**, 1333 (1977).
[4] S. E. Harris and J. C. White, IEEE J. Quantum Electron. **QE-13**, 972 (1977).
[5] A. Gallagher and T. Holstein, Phys. Rev. A **16**, 2413 (1977).
[6] S. Yeh and P. R. Berman, Phys. Rev. A **19**, 1106 (1979).
[7] M. G. Payne, V. E. Anderson, and J. E. Turner, Phys. Rev. A **20**, 1032 (1979).
[8] C. Brechignac, Ph. Cahuzac, and P. E. Toschek, Phys. Rev. A **21**, 1969 (1980).
[9] P. R. Berman, Phys. Rev. A **22**, 1838 (1980).
[10] A. Débarre, J. Phys. B **15**, 1693 (1982).
[11] A. Bambini and P. R. Berman, Phys. Rev. A **35**, 3753 (1987).
[12] S. Geltman, Phys. Rev. A **35**, 3775 (1987).
[13] M. Matera, M. Mazzoni, R. Buffa, S. Cavalieri, and E. Arimondo, Phys. Rev. A **36**, 1471 (1987).
[14] F. Dorsch, S. Geltman, and P. E. Toschek, Phys. Rev. A **37**, 2441 (1988).
[15] A. Agresti, P. R. Berman, A. Bambini, and A. Stefanel, Phys. Rev. A **38**, 2259 (1988).
[16] M. Matera, M. Mazzoni, M. Bianconi, R. Buffa, and L. Fini, Phys. Rev. A **41**, 3766 (1990).
[17] L. Fini, R. Buffa, R. Pratesi, A. Bambini, M. Matera, and M. Mazzoni (unpublished).
[18] R. Buffa and M. Matera, Phys. Rev. A **42**, 5709 (1990).
[19] A. Erdélyi, *Asymptotic Expansions* (Dover, New York, 1956), pp. 51–56.